Effect of photoinduced charge displacement on organic optoelectronic conversion

Laigui Hu,[1,2,*] Akito Iwasaki,[1] Rie Suizu,[1] Yukiko Noda,[1] Bo Li,[1,2] Hirofumi Yoshikawa,[1] Michio M. Matsushita,[1] Kunio Awaga,[1,3,†] and Hiroshi Ito[4]

[1]*Department of Chemistry and Research Center for Materials Science, Nagoya University, Chikusa-ku, Nagoya 464-8602, Japan*

[2]*Department of Applied Physics, Zhejiang University of Technology, Hangzhou 310023, China*

[3]*CREST, JST, Nagoya University, Chikusa-ku, Nagoya 464-8602, Japan*

[4]*Department of Applied Physics, Nagoya University, Chikusa-ku, Nagoya 464-8603, Japan*

(Received 21 February 2011; revised manuscript received 20 July 2011; published 21 November 2011)

As a significant drawback to organic electronics, poor mobility in organic materials makes it difficult for carriers to make long trips across thin film devices. In the present work, we show that a short carrier trip or even charge displacement can contribute to the functioning of optoelectronics without being influenced by the poor carrier mobility. Our findings are based on analysis of the current-voltage and capacitance-voltage characteristics, as well as the anomalous transient photocurrent of the photocells of a radical material, 4′4-bis(1,2,3,5-dithiadiazolyl). This photoinduced transient current was successfully analyzed based on the total current equation and was interpreted in terms of the polarization current induced by charge displacement in the films. This mechanism provides preliminary information with respect to the development of methods for high-speed organic optoelectronic conversion.

DOI: 10.1103/PhysRevB.84.205329 PACS number(s): 72.40.+w, 72.80.Le, 73.50.Pz, 73.61.Ph

I. INTRODUCTION

Organic optoelectronic devices including organic photovoltaics[1–3] and photodetectors[4–8] have received intense attention due to their flexibility, low cost, and ability to achieve large-area fabrication. However, the poor mobility of organic materials always gives rise to the formation of space charges in organic thin film devices, and the space charges limit both the conduction current and the photocurrent.[9] While most works on organic optoelectronics focus on improving device performance with a steady-state conduction current, a transient photocurrent (TPC)[10–13] has not been utilized, probably due to its ambiguous mechanism and characteristics.

We recently revealed an anomalous TPC in the thin film devices of 4′4-bis(1,2,3,5-dithiadiazolyl) (BDTDA)[14] and proposed that space charges stimulate this behavior. Such films consist of alternating one-dimensional π-stacking with molecular planes parallel to the substrates. The π-stacking can therefore bridge the distance between bottom and top electrodes, as shown in the inset of Fig. 1(a). As discussed in our previous work,[15] the lowest unoccupied molecular orbitals (LUMOs) of BDTDA form a wider band through the large overlap between the neighboring LUMOs, while the highest occupied molecular orbitals (HOMOs) form a narrow band. This difference leads to a significant carrier transport imbalance in the material. Due to the imbalance and the large thickness of the BDTDA films (∼300 nm), which naturally exceed the common carrier drift length in organic materials, space charges probably exist in the devices under illumination.[9]

The goal of the present study was to theoretically and experimentally explain the TPC of the BDTDA photocells based on the total current equation. We interpret the TPC in the BDTDA films in terms of a large polarization current induced by the formation of space charges near the electrodes of BDTDA thin film devices, which was confirmed by current-voltage (J-V) and capacitance-voltage (C-V) measurements. A space charge–limited current (SCLC) was observed, indicating an imbalance of carrier transport. Mott-Schottky plots for the C-V measurement demonstrate unwanted doping in the BDTDA films. The mechanism of the TPC appears to provide a potential mechanism for optoelectronics to utilize photoinduced charge displacement even without conduction current, especially for high-speed pulsed light organic detectors in various fields, such as optical communications and remote controls.

In this paper, the experimental methods are described and the results from J-V and C-V measurements are given to provide insight into the BDTDA film. A series of formulae based on the total current equation are then developed to fit the experimental data. The theoretical ideas behind this series are discussed in the final paragraph of Sec. III, and the final section gives a brief conclusion.

II. EXPERIMENT

Except for the radical BDTDA, all materials used in the present study were commercially available. The BDTDA was prepared as described in Ref. 16. Indium tin oxide (ITO) glass substrates were pretreated ultrasonically with 2-propanol, acetone, and chloroform. BDTDA thin films (300 nm) were thermally evaporated onto the substrates with a rate of 1 nm/s and under a vacuum pressure of $\sim 5 \times 10^{-4}$ Pa. Aluminum (Al) as a top electrode with a thickness of ∼50 nm was also thermally evaporated onto the thin films, and the effective area of the photocell was 0.02 cm^2. Film thickness was monitored by a quartz crystal microbalance.

Photocurrent and J-V measurements were carried out under a vacuum pressure of <1 Pa with the techniques described in Refs. 14 and 15. A Keithley 6487 picoammeter/voltage source was utilized as a power supply and current meter. To measure the photocurrent of the photocells, a monochromated 500-W halogen lamp with Nikon G250 grating was employed as a light source to irradiate the sample. The maximal monochromated light intensity in the visible region was ∼10 $\mu W/cm^2$, which was calibrated with a silicon (Si) photodiode.

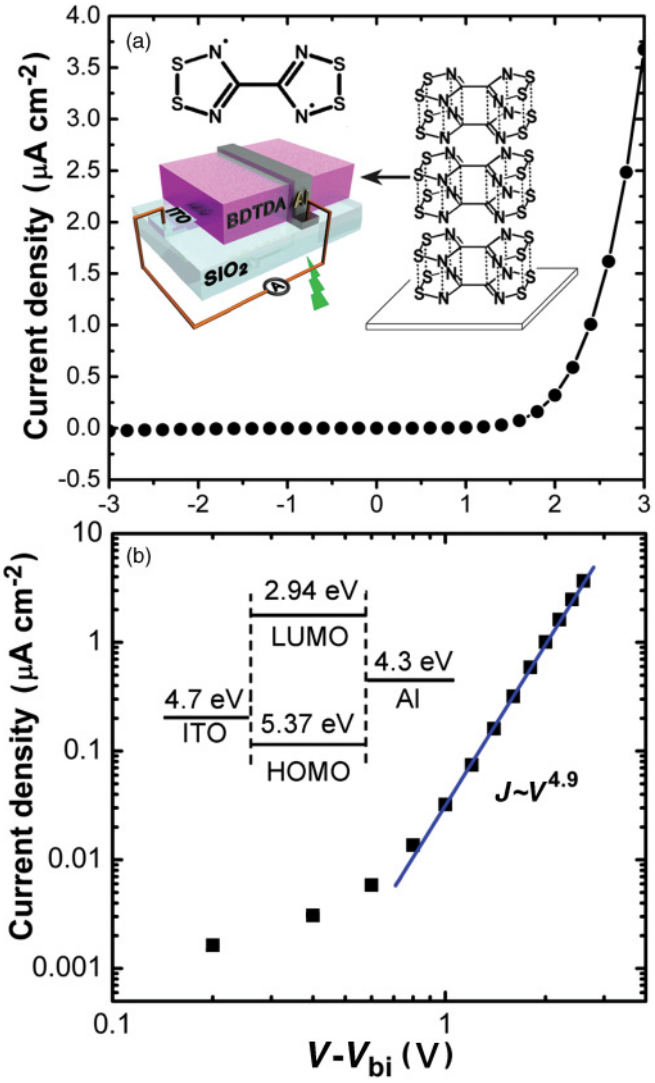

FIG. 1. (Color) The J-V characteristicsof a BDTDA photocell under a dark condition. (a) Linear plot of J versus V. The inset provides schematic views of the ITO/BDTDA/Al photocells and the molecular structure of BDTDA. (b) The log(J)–log(V) plot for the J-V curve in (a). The slope at high voltage (>0.8 V) is approximately 4.9. The inset shows an energy diagram for the ITO/BDTDA/Al photocell.

To match the absorption band of BDTDA thin films, light with a wavelength of 560 nm was chose and illuminated to the transparent ITO electrode. C-V characteristics of various devices were analyzed with an inductance–capacitance–resistance (LCR) meter (NF Electronic Instruments, ZM-2355). A direct current bias combined with a 0.1-V amplitude (root mean square value) alternating current signal was adopted at 100 Hz. Samples were fixed in a chamber filled with nitrogen.

III. RESULTS AND DISCUSSION

A. Space charge formation

To confirm the facility of the space charge formation in the ITO/BDTDA/Al photocells, the J-V characteristics were investigated under a dark condition. The Al electrode was grounded, and the bias polarity was defined as plus when a positive bias voltage was applied to ITO. Samples were fixed in a vacuum cryostat. The values of V were then scanned from −3 to 3 V. The J-V curve in Fig. 1(a) shows the rectification behavior, and the rectification rate can be estimated to be $\sim 10^2$ at ±2 V. This inferred behavior is reasonable, as the work functions of the two electrodes are different and noninjecting (see the energy diagram of electrodes and BDTDA in the inset of Fig. 1(b)).

The SCLC was analyzed using the J-V curve. The applied bias V was corrected[17] to compensate for the built-in voltage (V_{bi}) that mainly arises from the work function difference between the two electrodes. The voltage drop across the series resistance of BDTDA devices was not considered, as its value was very small. Figure 1(b) depicts the log (J)–log (V) plots, which are based on the data in Fig. 1(a). There are two regions in this curve with a crossover point ∼0.8 V. Below this crossover voltage, the J-V curve demonstrates Shockley behavior, which is ascribed to the injection limited current. At higher voltages ($V > 0.8$ V), the log (J)–log (V) plot exhibits a linear dependence, and its slope can be estimated to be ∼4.9. This value suggests that SCLC dominates this region, though the dependence does not satisfy Child's law ($J \propto V^2$).[18,19] Such bulk limited current can be ascribed to a trap-controlled SCLC or an SCLC with a field dependence of carrier mobility.[20,21] The space charges are therefore easily generated in the BDTDA thin film devices, mainly due to the significant imbalance of carrier transport and the relatively large thickness.

To check the distribution of space charges in the BDTDA thin film devices, C-V characteristics of an ITO/BDTDA (300 nm)/Al photocell device, with an effective area of 0.02 cm^2, were analyzed. The Mott-Schottky plot ($1/C^2$ versus V)[22] in Fig. 2(a) evidently demonstrates two linear regions. This indicates that the BDTDA film is not completely depleted. Taking into account that both blocking contacts will bring about two Schottky barriers connected in series, the barrier or junction with a much smaller capacitance C, which is determined by the space charge density and barrier height, should dominate the device capacitance. A narrow barrier width W of ∼2 nm for the first linear region, with a space charge density N of $\sim 10^{20}$ cm^{-3}, can be extracted based on the relations[23]

$$\frac{1}{C^2} = \frac{2}{A^2 q \varepsilon_0 \varepsilon_r N}(V_{bi} - V) \quad (1)$$

and

$$W = \sqrt{2\varepsilon_0 \varepsilon_r (V_{bi} - V)/qN}, \quad (2)$$

where A is the effective area; ε_0 and ε_r denote the dielectric constant of free space and the relative dielectric constant of the samples, respectively; and q means the elementary charge. The narrow width is probably related to surface states or a dipole layer. With the forward bias voltage increasing, such states are filled, and the capacitance is dominated by another barrier with $W \approx 10$ nm and $N \approx 10^{19}$ cm^{-3}.

To further characterize the barriers, a conductive poly(3,4-ethylenedioxythiophene) poly(styrenesulfonate) (PEDOT:PSS) film as an anode, with a work function of 5.2 eV, was spin coated onto a ITO glass. The corresponding device still demonstrates a positive slope in its Mott-Schottky

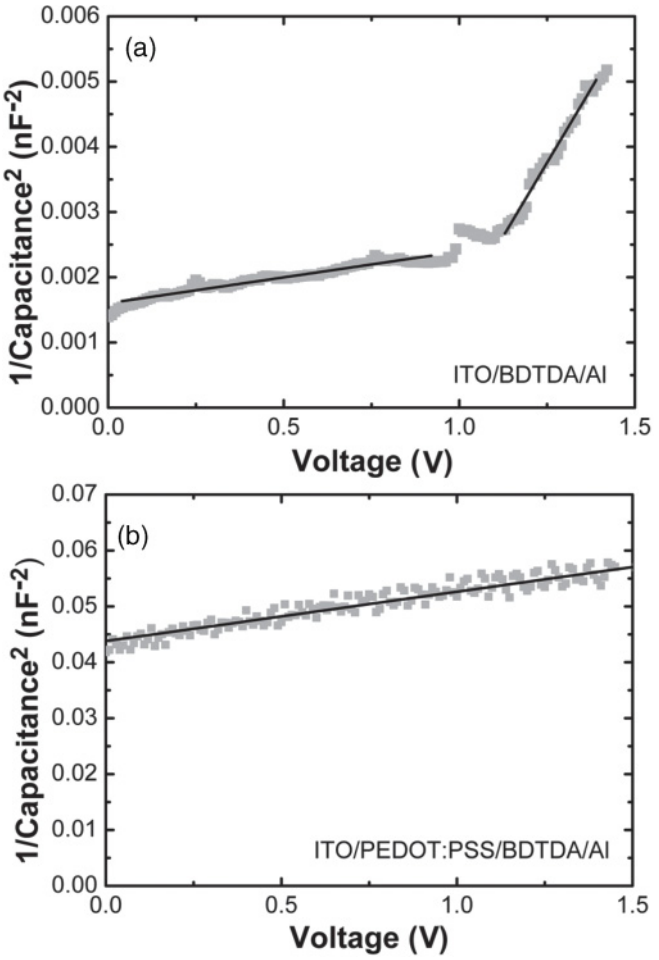

FIG. 2. (a) Mott-Schottky plot of the ITO/BDTDA (300 nm)/Al device. (b) Mott-Schottky plot of the Al/PEDOT:PSS/BDTDA (300 nm)/Al device.

plot, as shown in Fig. 2(b). N and W are calculated to be $\sim 10^{19}$ cm^{-3} and ~ 10 nm, respectively. This indicates that the conductive polymer may significantly improve the surface morphology of ITO and the surface states or dipole layer may be removed. The linearity in the Mott-Schottky plots evidently suggests that only one junction is dominant in the undepleted ITO/BDTDA/Al photocells and is responsible for the generation of photocurrent.

Considering that BDTDA may act as an n-type organic semiconductor,[15] the active region, with band bending for the generation of photocurrent, may exist near the interface of ITO/BDTDA (Fig. 3). Photogenerated excitons are mainly dissociated in the active region, and holes are collected by the ITO electrode, while electrons move in the opposite direction. However, the limitation of the electron drift length, due to relatively great thickness and a smaller electric field in bulk region, makes movement difficult; the electrons therefore accumulate near the border of the active region as photogenerated space charges. This induces a redistribution of the electric field and charge displacement inside the films.

Figure 4(a) shows the photoresponses of an ITO/BDTDA/Al photocell with a bias voltage of 0 V. Upon illumination of a monochromated light of 560 nm, a large TPC was collected followed by a steady-state

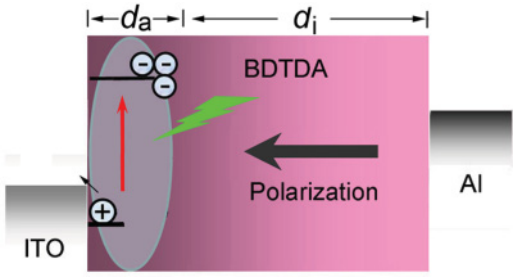

FIG. 3. (Color) Schematic view of the BDTDA photocells. Due to the large thickness and an imbalance of carrier transport, photogenerated space charges are accumulated at the boarder of the active layer (dark pink region). The built-in electric field will be changed, which leads to the generation of polarization current in the film.

photocurrent. Upon the removal of illumination, a negative TPC from Al to ITO in the external circuit appears. Both the TPC and steady-state photocurrent increase with increases in the light intensity. Figure 4(b) demonstrates the short circuit photoresponses under a reverse bias voltage of −2 V. As we can see, the TPC is dramatically suppressed. In particular, the negative current is nearly eliminated, while the steady-state current is increased. The corresponding photoresponsivity of the steady-state photocurrent under illumination of 1.81

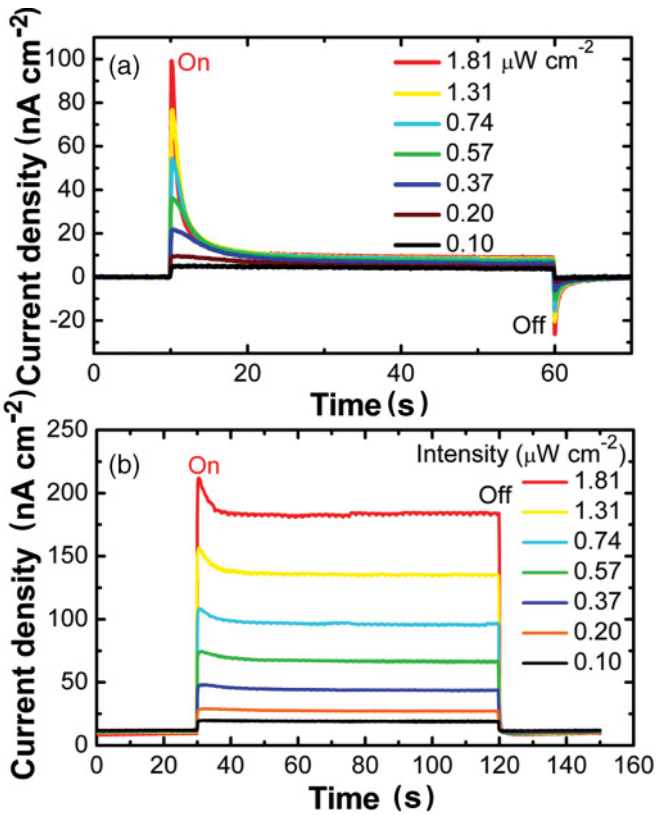

FIG. 4. (Color) Photoresponses of the BDTDA photocell with illumination of 560 nm. (a) Photoresponses under different light intensities with a zero bias voltage. Positive and negative anomalous TPC can be observed with the light on and off. (b) Photoresponses under different light intensities with a bias voltage of −2 V. Both positive and negative TPC were suppressed.

μW/cm^2 can approach 0.1 A/W. The TPC values under the zero bias can be comparable to those of the steady-state photocurrent under a bias voltage V. In addition, the positive TPC with a weak excitation light intensity ($\leqslant$0.57 μW/cm^2) decreases exponentially with time, and the decay time of the positive TPC shows light-intensity dependence. With stronger illumination, faster decay can be obtained. If the light intensity exceeds 0.57 μW/cm^2, the positive TPC cannot fit well with a single exponential simulation. This result may suggest that the TPC is a superposed signal with different mechanisms, including charge displacement triggered by the photoinduced space charges.

B. Theoretical analysis

We carried out a theoretical analysis to interpret the TPC in BDTDA photocells. Due to the existence of a junction with a width of d_a (dark pink region in Fig. 3) at the dominant interface (ITO/BDTDA) as an active region, which makes a different contribution to the TPC compared with the bulk region with a width of d_i (shallow pink region),[14] the thick film can be treated as a double-layer system.[24] By utilizing the total current equation, the photocurrent density J as a function of time t in external circuits (i.e., TPC) can be expressed as[25]

$$J(t) = \frac{\xi}{(\tau - RC)}\left(e^{-\frac{t}{\tau}} - e^{-\frac{t}{RC}}\right), \tag{3}$$

where $\xi = \varepsilon_0{\varepsilon_i}^2 d_a V \,/\, d_i(d_i\varepsilon_a + d_a\varepsilon_i)$ and $\tau = \varepsilon_0(d_i\varepsilon_a + d_a\varepsilon_i) \,/\, d_i{\sigma_a}^*$. ε_i and ε_a denote the relative dielectric constants of the bulk region and the junction region, respectively. ${\sigma_a}^*$ is the photoconductivity in the junction region. RC is a time constant in the circuit. Based on Eq. (3), we successfully simulated the TPC, as shown in Fig. 5. The positive TPC at 0.2 μW/cm^2 exhibits a large τ (9.4 s) and a much smaller RC time constant (0.3 s).

We consider the situation of weak illumination. Since ${\sigma_a}^* = \phi I$, where I refers to the light intensity and ϕ is a proportional constant, the decay time of the first term in Eq. (3) can be written as

$$\tau = \frac{\varepsilon_0(d_i\varepsilon_a + d_a\varepsilon_i)}{d_i\phi I}, \tag{4}$$

which suggests a relationship of $\tau \propto I^{-1}$. Therefore, weak illumination leads to a large τ. If $\tau \gg RC$, and Eq. (3) changes to

$$J \approx J_m e^{-\frac{t}{\tau}}, \tag{5}$$

with a maximal $J(t)$ value J_m:

$$J_m = \frac{\xi d_i \phi I}{\varepsilon_0(d_i\varepsilon_a + d_a\varepsilon_i)} \propto I. \tag{6}$$

Equation (5) suggests that the TPC exhibits an exponential decay under weak irradiation and/or with a very small RC time constant in circuit, which fits well with the experimental behavior.

To check Eqs. (4) and (6), the time decay τ and J_m were extracted from Fig. 4(a) and plotted in Fig. 6 (square points).

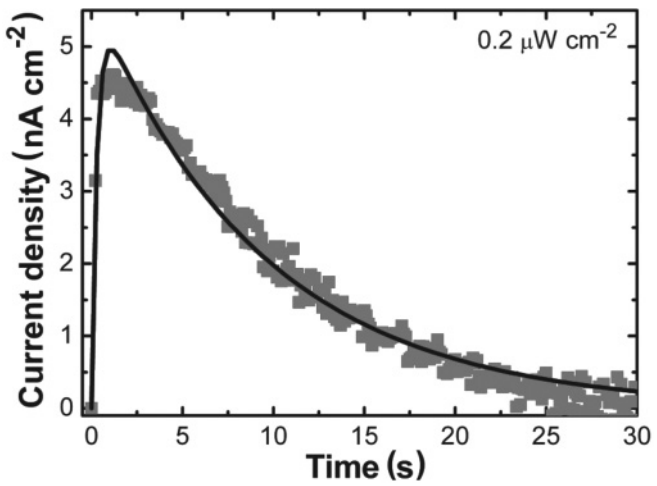

FIG. 5. Curve fitting (solid curve) for the positive TPC under illumination of 0.2 μW/cm^2 (square points) based on Eq. (3), which shows good agreement.

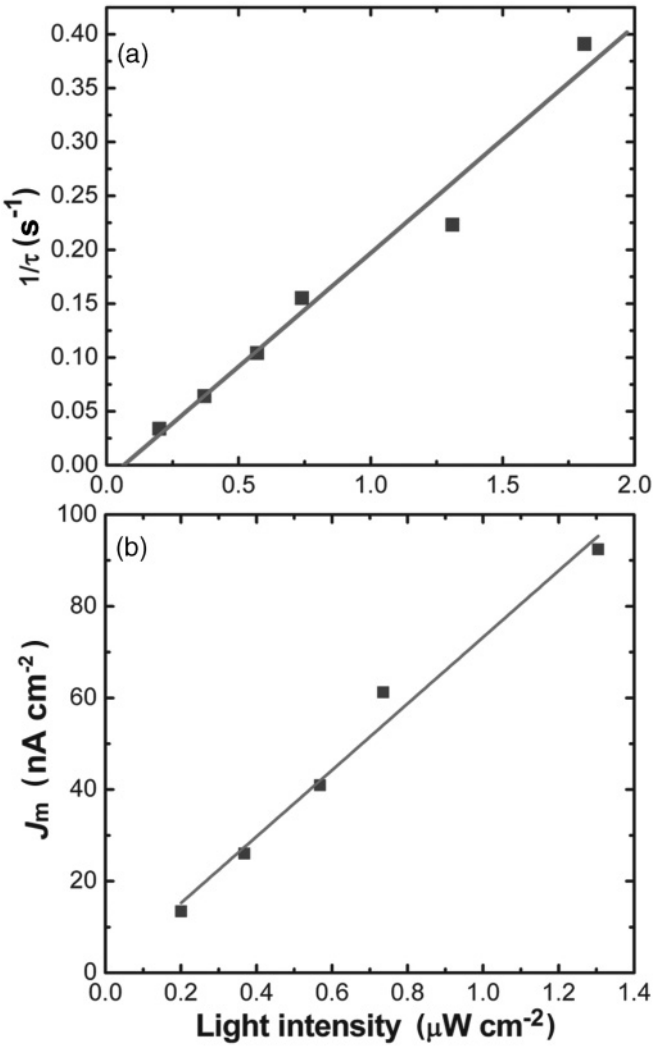

FIG. 6. (a) Light-intensity dependence of the decay time of positive TPC with illumination from a monochromated light of 560 nm. The decay time linearly decreases with the intensity. (b) Light-intensity dependence of the peak value of TPC, which exhibits linearity as the prediction in Eq. (6). Square points are the experimental data extracted from Fig. 4(a).

As we can see from Fig. 6(a), the decay time of the positive TPC under different illuminations shows light-intensity dependence. The time linearly decreases with increases in the light intensity ($\tau \propto I^{-1}$). Therefore, a large light intensity can shorten the time for the generation of photoinduced space charges. Figure 6(b) shows the relationship between light intensity and peak value J_m. The linearity exhibits good agreement with the prediction from Eq. (6), i.e., $J_m \propto I$.

C. Mechanism of anomalous TPC

The results of the theoretical analysis match well with our experimental data, suggesting that the TPC in BDTDA involves two mechanisms, i.e., the conduction current in the thin junction region and the displacement current due to polarization mainly in the bulk region. The anomalous behavior is universal for the thin films with large polarity, poor mobility, relatively large thickness. In our analysis, the variation in the dielectric constant induced by space charges was omitted for simplification, which may also contribute to the displacement component in the TPC. Though the carriers in organic materials cannot withstand a long trip due to various means of dissipation, including traps and recombination, displacement or a polarization current can generate a large TPC without a long trip. Fast generation of this photocurrent is possible because the photoinduced polarization current allows localized charges to oscillate around their equilibrium states. These results suggest that photoactive materials in an electric field, including photorefractive and photoisomerization materials, may also exhibit the TPC even without the conduction photocurrent. In addition, the faster photoinduced changes of a built-in electric field or dielectric constant lead to a larger TPC. A high speed may be achieved since the performance is mainly limited by the fast dielectric relaxation,[26] not the conventional effect, i.e., slow carrier transit process. These are promising for high-speed operation in organic optoelectronics.

IV. CONCLUSION

We have experimentally and theoretically analyzed the anomalous TPC in BDTDA photocells with a thickness of 300 nm. A series of theoretical formulae for the TPC based on the total current equation were developed. The theoretical simulations of TPC peak profiles, decay time, and light-intensity dependence match the experimental data well. The polarization current triggered by the photoinduced space charges plays a significant role in the TPC, in addition to the conventional time-dependent conduction photocurrent. Though a lack of mobility is the main drawback to using organic materials for conduction, the poor mobility does not hamper the polarization current. Therefore, the photoinduced polarization/displacement current is quite applicable to use in high-speed organic optoelectronic devices.

ACKNOWLEDGMENTS

This research was supported by a grant-in-aid for scientific research from the Ministry of Education, Culture, Sports, Science, and Technology. L.H. also thanks the National Natural Science Foundation of China (Grants No. 11004172 and No. 10804098).

*hu.laigui@g.mbox.nagoya-u.ac.jp
†awaga@mbox.chem.nagoya-u.ac.jp

[1] P. Peumans, S. Uchida, and S. R. Forrest, Nature **425**, 158 (2003).
[2] M. R. Lee, R. D. Eckert, K. Forberich, G. Dennler, C. J. Brabec, and R. A. Gaudiana, Science **324**, 232 (2009).
[3] K. V. Chauhan, P. Sullivan, J. L. Yang, and T. S. Jones, J. Phys. Chem. C **114**, 3304 (2010).
[4] G. Konstantatos, J. Clifford, L. Levina, and E. H. Sargent, Nat. Photon. **1**, 531 (2007).
[5] M. Binda, T. Agostinelli, M. Caironi, D. Natali, M. Sampietro, L. Beverina, R. Ruffo, and F. Silvestri, Org. Electron. **10**, 1314 (2009).
[6] G. Matsunobu, Y. Oishi, M. Yokoyama, and M. Hiramoto, Appl. Phys. Lett. **81**, 1321 (2002).
[7] T. Morimume, H. Kajii, and Y. Ohmori, IEEE Photon. Tech. Lett. **18**, 2662 (2006).
[8] W. W. Tsai, Y. C. Chao, E. C. Chen, H. W. Zan, H. F. Meng, and C. S. Hsu, Appl. Phys. Lett. **95**, 213308 (2009).
[9] V. D. Mihailetchi, J. Wildeman, and P. W. M. Blom, Phys. Rev. Lett. **94**, 126602 (2005).
[10] A. Kumar, S. Goel, and D. S. Misra, Phys. Rev. B **35**, 5635 (1987).
[11] K. Tahira and K. C. Kao, J. Phys. D Appl. Phys. **18**, 2247 (1985).
[12] A. M. Andriesh, V. I. Arkhipov, M. S. Iovu, A. I. Rudenko, and S. D. Shutov, Solid State Comm. **48**, 1041 (1983).
[13] A. Sugimura, H. Sonomura, H. Naito, and M. Okuda, Phys. Rev. Lett. **63**, 555 (1989).
[14] L. G. Hu, A. Iwasaki, R. Suizu, H. Yoshikawa, K. Awaga, and H. Ito, Chem. Phys. Lett. **484**, 177 (2010).
[15] A. Iwasaki, L. G. Hu, R. Suizu, K. Nomura, H. Yoshikawa, K. Awaga, Y. Noda, K. Kanai, Y. Ouchi, K. Seki, and H. Ito, Angew. Chem. Int. Ed. **48**, 4022 (2009).
[16] C. D. Bryan, A. W. Cordes, J. D. Goddard, R. C. Haddon, R. G. Hicks, C. D. MacKinnon, R. C. Mawhinney, R. T. Oakley, T. T. M. Palstra, and A. S. Perel, J. Am. Chem. Soc. **118**, 330 (1996).
[17] J. K. J. van Duren, V. D. Mihailetchi, P. W. M. Blom, T. van Woudenbergh, J. C. Hummelen, M. T. Rispens, R. A. J. Janssen, and M. M. Wienk, J. Appl. Phys. **94**, 4477 (2003).
[18] N. Karl, Synth. Met. **133**, 649 (2003).
[19] V. Coropceanu, J. Cornil, D. A. da Silva, Y. Olivier, R. Silbey, and J. L. Bredas, Chem. Rev. **107**, 926 (2007).
[20] G. D. Sharma, Synth. Met. **74**, 227 (1995).
[21] P. W. M. Blom, M. J. M. deJong, and M. G. vanMunster, Phys. Rev. B **55**, R656 (1997).
[22] P. Stallinga, H. L. Gomes, M. Murgia, and K. Mullen, Org. Electron. **3**, 43 (2002).
[23] P. Stallinga, *Electrical Characterization of Organic Electronic Materials and Devices* (John Wiley & Sons, Chichester, United Kingdom, 2009).
[24] L. G. Hu, Y. Noda, H. Ito, H. Kishida, A. Nakamura, and K. Awaga, Appl. Phys. Lett. **96**, 243303 (2010).
[25] See Supplemental Material at http://link.aps.org/supplemental/10.1103/PhysRevB.84.205329 for the derivation of the formula.
[26] K.-C. Kao, *Dielectric Phenomena in Solids* (Elsevier Academic Press, Amsterdam, 2004).